



**HAL**  
open science

## Modelling the magnetic dipole

Kira Seleznyova, Mark Strugatsky, Janis Kliava

► **To cite this version:**

Kira Seleznyova, Mark Strugatsky, Janis Kliava. Modelling the magnetic dipole. *European Journal of Physics*, 2016, 37 (2), pp.025203 (1-14). 10.1088/0143-0807/37/2/025203 . hal-01275891

**HAL Id: hal-01275891**

**<https://hal.science/hal-01275891>**

Submitted on 18 Feb 2016

**HAL** is a multi-disciplinary open access archive for the deposit and dissemination of scientific research documents, whether they are published or not. The documents may come from teaching and research institutions in France or abroad, or from public or private research centers.

L'archive ouverte pluridisciplinaire **HAL**, est destinée au dépôt et à la diffusion de documents scientifiques de niveau recherche, publiés ou non, émanant des établissements d'enseignement et de recherche français ou étrangers, des laboratoires publics ou privés.



Distributed under a Creative Commons Attribution - ShareAlike 4.0 International License

# Modelling the magnetic dipole

Kira Seleznyova<sup>1,2</sup>, Mark Strugatsky<sup>2</sup> and Janis Kliava<sup>1</sup>

<sup>1</sup>LOMA, UMR 5798 Université de Bordeaux CNRS, F 33405 Talence cedex, France

<sup>2</sup>Physics and Technology Institute, Crimean Federal V.I. Vernadsky University, Simferopol, Republic of Crimea

E mail: [janis.kliava@u-bordeaux.fr](mailto:janis.kliava@u-bordeaux.fr)

## Abstract

Three different models of a magnetic dipole, viz., a uniformly magnetised sphere, a circular current loop and a pair of fictitious magnetic charges, have been systematically analysed within the formalism based on the vector potential of the magnetic field. The expressions of the potentials and magnetic fields produced by each dipole model have been obtained. A computer code has been put forward in order to visualise magnetic field lines for different dipole models. It has been shown that the magnetic field outside the uniformly magnetised sphere coincides with that of a point dipole. The other two models give considerably different results at distances small or intermediate in comparison with the dipole size.

Keywords: magnetic dipole, uniformly magnetised sphere, circular current loop, pair of magnetic monopoles, magnetic field lines

## 1. Introduction

In electrostatics, the primary source of the electric field is an electric charge. In contrast, in magnetostatics, insofar as ‘magnetic charges’ magnetic monopoles have not been found in nature, the same fundamental role of primary source of the magnetic field is played by the magnetic dipole. Therefore, adequate modelling of the magnetic dipole is of paramount importance, both in teaching and scientific research.

As far as a *point* dipole is only an abstract idea, in teaching magnetostatics as well as in research in the field of magnetism, it is useful to consider dipole models more realistic physical systems yielding the same magnetic field as the point dipole, at least, at distances much larger than their own size. Most often, as such a model in magnetostatics one considers a circular current loop or, by analogy with electrostatics, a pair of *fictitious* magnetic charges

of opposite sign. Meanwhile, there is the third possibility, that to model the magnetic dipole as a *uniformly* magnetised three-dimensional body of a simple, e.g., spherical shape. Usually, the uniformly magnetised sphere is considered in a different context, viz., as an illustration of a boundary-value problem in magnetostatics [1, p 198 ff], or an example of application of the vector potential [2, p 236], thus overlooking the opportunity of using it as one more model of the magnetic dipole. Below we shall compare in detail all three dipole models.

Of course, the magnetic field produced by a dipole model at intermediate and shorter distances will differ from that of the point dipole; moreover, the predictions of different models can be quite different. This issue is of importance, e.g., in studying magnetic dipole-dipole interactions between paramagnetic ions in solid state, in which case a comparison with experimental observations allows choosing the most adequate description of a given magnetic source.

In teaching electromagnetism, the analogy between electrostatics and magnetostatics suggests that the electric and the magnetic dipole should be introduced in an analogous manner. This can be implemented in two different ways: (i) by calculating the electric and magnetic dipole fields through the Coulomb and Biot-Savart laws, respectively and (ii) by deriving them from scalar and vector potentials, respectively. The first way has been explored in detail by Bezerra *et al* [3]. We have chosen the second way, more sophisticated from the conceptual viewpoint but allowing to considerably simplify certain computations.

In one form or another, the models considered below have been described in a number of textbooks and/or research papers. Meanwhile, we have tried to present them systematically within the same formalism and comparing exact analytical expressions with Taylor expansions to higher-than-first order, providing simple expressions of potentials and fields valid not only at large but also at intermediate distances. A computer code has been put forward, allowing to visualise magnetic field lines computed using both exact expressions and Taylor expansions.

We believe that this paper will be interesting and useful to people involved in teaching both undergraduate and graduate courses as well as in research work in the field of electromagnetism.

## 2. Point dipole: an overview

According to the Biot-Savart law of magnetostatics, the magnetic field  $\mathbf{B}(\mathbf{r})$  produced in a point of space  $\mathbf{r} = (x, y, z)$  by an arbitrary distribution of steady currents in a volume  $V'$  is (e.g., see [1, p 175 ff], [2, p 215 ff]):

$$\mathbf{B}(\mathbf{r}) = \frac{\mu_0}{4\pi} \int_{V'} \frac{\mathbf{j}(\mathbf{r}') \wedge (\mathbf{r} - \mathbf{r}')}{|\mathbf{r} - \mathbf{r}'|^3} dV'. \quad (1)$$

The same expression is obtained with the help of the relation  $\mathbf{B}(\mathbf{r}) = \nabla \wedge \mathbf{A}(\mathbf{r})$ ,  $\mathbf{A}(\mathbf{r})$  being the corresponding vector potential:

$$\mathbf{A}(\mathbf{r}) = \frac{\mu_0}{4\pi} \int_{V'} \frac{\mathbf{j}(\mathbf{r}')}{|\mathbf{r} - \mathbf{r}'|} dV'. \quad (2)$$

In equations (1) and (2)  $\mu_0$  is the permeability of vacuum,  $\mathbf{j}(\mathbf{r}')$  is the current density in a point  $\mathbf{r}' = (x', y', z')$  of the magnetic source, and the integration is performed over the whole distribution of currents. The corresponding analysis, outlined below, can be found, e.g., in Jackson's and Landau and Lifshitz's textbooks ([1, p 184 ff], [4, p 103 ff]).

Equation (2) can be expanded in powers of  $r^{-1}$  (the multipole expansion):

$$\mathbf{A}(\mathbf{r}) = \frac{\mu_0}{4\pi} \frac{1}{r^{n+1}} \sum_{n=0}^{\infty} \int_{V'} r'^n \mathbf{j}(\mathbf{r}') P_n(\cos \alpha) dV', \quad (3)$$

where  $P_n$  are the Legendre polynomials and  $\alpha$  is the angle between  $\mathbf{r}$  and  $\mathbf{r}'$ . The first term of this development ( $n = 0$ )

$$\mathbf{A}_m = \frac{\mu_0}{4\pi r} \int_{V'} \mathbf{j}(\mathbf{r}') dV', \quad (4)$$

is the vector potential of the magnetic monopole,  $\mathbf{A}_m$ , and it is shown to vanish. The second term in equation (3),  $n = 1$ , the magnetic dipole term

$$\mathbf{A}_d = \frac{\mu_0}{4\pi r^3} \int_{V'} (\mathbf{r} \cdot \mathbf{r}') \mathbf{j}(\mathbf{r}') dV', \quad (5)$$

can be put in the following form:

$$\mathbf{A}_d = -\frac{\mu_0}{4\pi} \mathbf{m} \wedge \nabla \frac{1}{r}, \quad (6)$$

where  $\mathbf{m}$  is the magnetic dipole moment:

$$\mathbf{m} = \frac{1}{2} \int_{V'} \mathbf{r}' \wedge \mathbf{j}(\mathbf{r}') dV'. \quad (7)$$

Taking the curl of  $\mathbf{A}_d$ , applying the product rule and keeping in mind that  $\mathbf{m}$  is a fixed vector, for the magnetic field produced by a point dipole one gets:

$$\mathbf{B}_d = \frac{\mu_0}{4\pi} \frac{3(\mathbf{m} \cdot \mathbf{r})\mathbf{r} - r^2 \mathbf{m}}{r^5}. \quad (8)$$

According to the Curie symmetry principle [5], the effects generated by a cause can have only *higher* and not *lower* symmetry than the cause itself. We put the dipole at the origin  $O$  (in subsequent sections,  $O$  will be chosen in the centre of the dipole model). As far as the dipole field is invariant with respect to rotation about its axis denoted as  $Oz$ , the use of cylindrical coordinates  $\rho, \varphi, z$  and the corresponding unit vectors  $\mathbf{e}_\rho, \mathbf{e}_\varphi, \mathbf{e}_z$  is the most appropriate, and all calculations can be restricted to a plane containing  $Oz$ . The position of a point in this plane can be defined either by the radius  $r$  and the polar angle  $\vartheta$  or by the distance  $\rho = r \sin \vartheta$  and the height  $z = r \cos \vartheta$ ; below we are thoroughly using the former definition. Thus, equations (6) and (8) become:

$$\mathbf{A}_d = \frac{\mu_0}{4\pi} \frac{m}{r^2} \sin \vartheta \mathbf{e}_\varphi \quad (9)$$

and

$$\mathbf{B}_d = \frac{\mu_0}{4\pi} \frac{m}{r^3} \left[ \frac{3}{2} \sin 2\vartheta \mathbf{e}_\rho + (3 \cos^2 \vartheta - 1) \mathbf{e}_z \right]. \quad (10)$$

### 3. Uniformly magnetised sphere

The magnetic field produced by a uniformly magnetised sphere, see figure 1, has been addressed, e.g., in [1, p 198 ff]. A related model, that of a spinning spherical shell carrying a uniform surface charge, has been treated in the Griffith's textbook [2, p 236 ff].

We consider the magnetised sphere of radius  $R$  and magnetic dipole moment  $\mathbf{m} = \frac{4}{3}\pi R^3 \mathbf{M}$  where  $\mathbf{M}$  is the magnetisation vector supposed to be uniform, as an assembly of

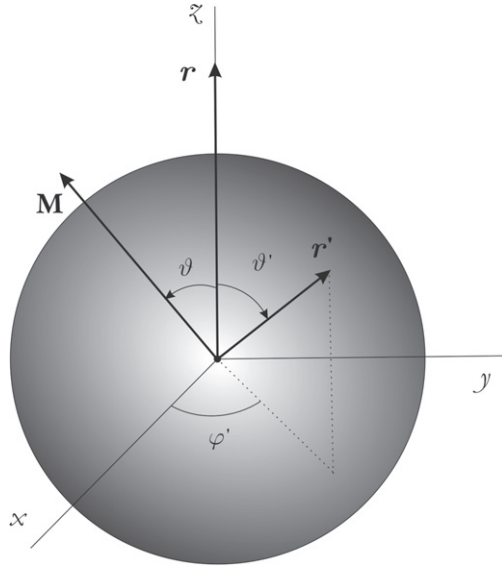


**Figure 1.** Magnetic dipole modelled by a uniformly magnetised sphere.

elementary dipoles. Taking into account equation (6), the vector potential produced by such a sphere in a point of radius vector  $\mathbf{r}$  can be calculated as a sum of contributions of all volume elements  $dV'$  of radius vector  $\mathbf{r}'$  and dipole moment  $d\mathbf{m} = \mathbf{M}dV'$ :

$$\mathbf{A} = -\frac{\mu_0}{4\pi} \int_{V'} \mathbf{M} \wedge \nabla' \frac{1}{|\mathbf{r} - \mathbf{r}'|} dV'. \quad (11)$$

For a uniform  $\mathbf{M}$ , the latter expression can be rewritten as

$$\mathbf{A} = -\frac{\mu_0}{4\pi} \int_{V'} \nabla' \wedge \frac{\mathbf{M}}{|\mathbf{r} - \mathbf{r}'|} dV'. \quad (12)$$

In accordance with a well-known theorem of vector analysis, the volume integral in this expression can be transformed to an integral over the surface  $S'$  of the sphere:

$$\mathbf{A}(\mathbf{r}) = \frac{\mu_0}{4\pi} \oint_{S'} \frac{\mathbf{M} \wedge \mathbf{n}}{|\mathbf{r} - \mathbf{r}'|} dS', \quad (13)$$

where  $\mathbf{n} = \mathbf{r}'/r'$  is the unit vector normal to  $S'$  and  $dS' = R^2 \sin \vartheta' d\vartheta' d\varphi'$ . A comparison between equations (2) and (13) shows that the latter describes the vector potential of a surface current of density  $\mathbf{j}_S(\mathbf{r}') = \mathbf{M} \wedge \mathbf{n}$ .

We choose the space origin in the centre of the sphere and the  $z$  axis parallel to  $\mathbf{r}$ ,  $\mathbf{r} = r \mathbf{e}_z$  (such a choice allows simplifying the calculation, see [2, p 236 ff]). One can see from figure 1 that  $\mathbf{r}' = R(\sin \vartheta' \cos \varphi', \sin \vartheta' \sin \varphi', \cos \vartheta')$  and  $|\mathbf{r} - \mathbf{r}'| = (r^2 + R^2 - 2rR \cos \vartheta')^{1/2}$ . Because of the rotational symmetry about  $\mathbf{M}$ , without loss of generality  $\mathbf{M}$  can be confined in the  $xz$  plane, forming an angle  $\vartheta$  with  $\mathbf{r}$ ,  $\mathbf{M} = M(\sin \vartheta, 0, \cos \vartheta)$ , so that

$$\begin{aligned} \mathbf{M} \wedge \mathbf{n} = M &(-\sin \vartheta' \sin \varphi' \cos \vartheta, \sin \vartheta' \cos \varphi' \cos \vartheta \\ & - \cos \vartheta' \sin \vartheta, \sin \vartheta' \sin \varphi' \sin \vartheta). \end{aligned} \quad (14)$$

Making these substitutions in equation (13), we remark that integrating over the range  $0 \leq \varphi' < 2\pi$  will eliminate contributions of all  $\varphi'$ -dependent terms in equation (14). The remaining integral over  $\vartheta'$  yields:

$$\mathbf{A} = \begin{cases} \frac{\mu_0}{4\pi} \frac{mr}{R^3} \sin \vartheta \mathbf{e}_\varphi, & r \leq R, \\ \frac{\mu_0}{4\pi} \frac{m}{r^2} \sin \vartheta \mathbf{e}_\varphi, & r \geq R. \end{cases} \quad (15)$$

Taking the curl of  $\mathbf{A}$  inside and outside the sphere, we get the corresponding magnetic fields  $\mathbf{B}^{\text{int}}$  and  $\mathbf{B}^{\text{ext}}$  in cylindrical coordinates:

$$\begin{aligned} \mathbf{B}^{\text{int}} &= 2 \frac{\mu_0}{4\pi} \frac{m}{R^3} \mathbf{e}_z, \\ \mathbf{B}^{\text{ext}} &= \frac{\mu_0}{4\pi} \frac{m}{r^3} \left[ \frac{3}{2} \sin 2\vartheta \mathbf{e}_\rho + (3 \cos^2 \vartheta - 1) \mathbf{e}_z \right]. \end{aligned} \quad (16)$$

One can see that inside the uniformly magnetised sphere the magnetic field is uniform, as known from magnetostatics. Most interestingly, outside this sphere the magnetic field at any distance coincides with that of the point dipole, see equations (16) and (10).

#### 4. Circular current loop

Most often, in magnetostatics one takes a circular loop of electric current (Ampérian current) as a basic model of the magnetic dipole. Let us consider a loop of radius  $R$  and area  $S = \pi R^2$ , placed in the  $xy$  plane and centred at the origin, see figure 2. The loop is carrying a current  $I$  supposed to flow in counterclockwise direction as seen from above the  $xy$  plane; so, by definition, its magnetic moment is  $m = \pi R^2 I$ . An element of current  $I d\mathbf{l}$ , where  $d\mathbf{l}$  is an elementary vector tangent to the loop in a point  $M$ , produces an elementary vector potential in an arbitrary point in space  $P$ :

$$d\mathbf{A} = \frac{\mu_0}{4\pi} \frac{m}{\pi R^2} \frac{d\mathbf{l}}{|MP|}. \quad (17)$$

Because of rotational symmetry about the  $z$  axis, without loss of generality  $P$  can be positioned in the  $yz$  plane. In polar coordinates we get  $d\mathbf{l} = R d\varphi' \mathbf{e}_\varphi$ . From figure 2 one can see that  $\overline{MP} = \overline{MO} + \overline{OP}$  and  $|MP| = \sqrt{r^2 + R^2 - 2Rr \sin \vartheta \sin \varphi'}$ .

In performing the integration of  $d\mathbf{A}$  over the current loop,  $d\mathbf{l}$  should be converted to Cartesian coordinates by substituting  $\mathbf{e}_\varphi = -\sin \varphi' \mathbf{e}_x + \cos \varphi' \mathbf{e}_y$ . Thus

$$\mathbf{A} = \frac{\mu_0}{4\pi} \frac{m}{\pi R} \int_0^{2\pi} \frac{-\sin \varphi' \mathbf{e}_x + \cos \varphi' \mathbf{e}_y}{\sqrt{r^2 + R^2 - 2Rr \sin \vartheta \sin \varphi'}} d\varphi'. \quad (18)$$

It turns out that  $A_y = 0$ . Identifying  $A_x$  as  $-A_\varphi$ , and denoting  $r_\pm^2 = r^2 + R^2 \pm 2Rr \sin \vartheta$  and  $k = 2\sqrt{Rr \sin \vartheta} / r_+$ , we get:

$$\mathbf{A} = \frac{\mu_0}{4\pi} \frac{8m}{\pi R k^2 r_+} \left[ \left( 1 - \frac{1}{2} k^2 \right) K(k) - E(k) \right] \mathbf{e}_\varphi \quad (19)$$

where  $K(k)$  and  $E(k)$  are, respectively, complete elliptic integrals of the first and second kind. From this equation we derive the cylindrical components of the magnetic field vector:

$$\begin{aligned} B_\rho &= \frac{\mu_0}{4\pi} \frac{2m}{\pi R^2 r_+ r_-^2} \cot \vartheta [(r^2 + R^2) E(k) - r_-^2 K(k)], \\ B_z &= \frac{\mu_0}{4\pi} \frac{2m}{\pi R^2 r_+ r_-^2} [(R^2 - r^2) E(k) - r_+^2 K(k)]. \end{aligned} \quad (20)$$



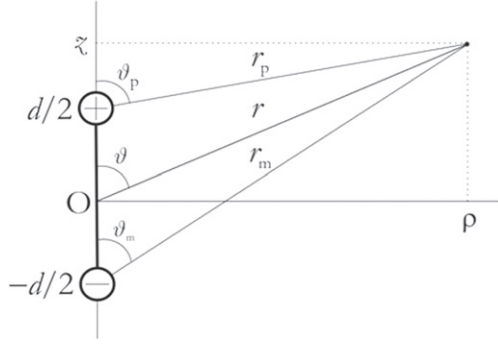


**Figure 3.** Magnetic dipole modelled by an assembly of two ‘magnetic charges’.

standpoints, as far as it exhibits a singularity along the half-line  $\vartheta = \pi$  (the so-called Dirac string); while for a magnetic monopole the direction of this half-line is completely arbitrary. Meanwhile, it can be readily shown that the vector potential of a pair of magnetic monopoles of opposite signs,

$$\mathbf{A} = \frac{\mu_0 m}{4\pi d} \left( \frac{1 - \cos \vartheta_p}{r_p \sin \vartheta_p} - \frac{1 - \cos \vartheta_m}{r_m \sin \vartheta_m} \right) \mathbf{e}_\varphi, \quad (24)$$

has no more such singularities. The latter equation can be rewritten as:

$$\mathbf{A} = \frac{\mu_0 m}{4\pi r d \sin \vartheta} \left( \frac{r \cos \vartheta + \frac{1}{2}d}{r_m} - \frac{r \cos \vartheta - \frac{1}{2}d}{r_p} \right) \mathbf{e}_\varphi, \quad (25)$$

where the connotation of different symbols is shown in figure 3. Obviously, the following relations hold:  $r_{p,m} = \sqrt{r^2 \mp dr \cos \vartheta + \frac{1}{2}d^2}$ ,  $\cos \vartheta_{p,m} = \frac{r \cos \vartheta \mp \frac{1}{2}d}{r_{p,m}}$  (the upper and lower signs corresponding to the first and second subscripts, respectively) and  $r_{p,m} \sin \vartheta_{p,m} = r \sin \vartheta$ .

For the magnetic field components we get:

$$\begin{aligned} B_\rho &= \frac{\mu_0 m}{4\pi d} r \sin \vartheta \left( \frac{1}{r_p^3} - \frac{1}{r_m^3} \right), \\ B_z &= \frac{\mu_0 m}{4\pi d} \left( \frac{r \cos \vartheta - \frac{1}{2}d}{r_p^3} - \frac{r \cos \vartheta + \frac{1}{2}d}{r_m^3} \right). \end{aligned} \quad (26)$$

Note that the latter equations can be immediately obtained from the corresponding expressions for the electric dipole by substituting the electric dipole moment and the permittivity of vacuum  $\varepsilon_0$  by the magnetic dipole moment and  $\mu_0^{-1}$ , respectively. These expressions are simpler in comparison with those obtained for the model of a current loop. Yet, we still provide the corresponding expansions in the Taylor series, useful for a direct comparison between these two models. In the same approximation as in the previous section, redefining the small parameter as  $\varepsilon = d/r$ , equations (25) and (26) become, respectively:

$$\mathbf{A} = -\frac{\mu_0 m}{4\pi r^2} \left( P_1^1 + \frac{1}{12} P_3^1 \varepsilon^2 + \frac{1}{80} P_5^1 \varepsilon^4 + \frac{1}{448} P_7^1 \varepsilon^6 \right) \mathbf{e}_\varphi \quad (27)$$

and

$$\begin{aligned} B_\rho &= -\frac{\mu_0 m}{4\pi r^3} \left( P_2^1 + \frac{1}{4} P_4^1 \varepsilon^2 + \frac{1}{16} P_6^1 \varepsilon^4 + \frac{1}{64} P_8^1 \varepsilon^6 \right), \\ B_z &= \frac{\mu_0 m}{4\pi r^3} \left( 2P_2^1 + P_4^1 \varepsilon^2 + \frac{3}{8} P_6^1 \varepsilon^4 + \frac{1}{8} P_8^1 \varepsilon^6 \right). \end{aligned} \quad (28)$$

## 6. Comparison between the dipole models

Figure 4 compares radial dependences of  $B_z$  in the equatorial plane  $\vartheta = \pi/2$  for different dipole models. The calculations have been made using the exact expressions for  $B_z$ . The model sizes and the distances are scaled in relative distance units (rdu). As one can see, for the uniformly magnetised sphere of radius  $R$ ,  $B_z$  remains uniform at  $\rho < R$ , has a discontinuity at  $\rho = R$  and follows the corresponding dependence for the point dipole at  $\rho > R$ . The analogous dependence for the current loop of radius  $R$  has a singularity at  $\rho = R$ , and for the pair of magnetic charges  $B_z$  has a minimum at  $\rho = 0$ . Thus, at small and intermediate distances in comparison with the model size, the behaviour of all three models is very different. At large distances, see inset in figure 4, the magnetic fields produced by different magnetic dipole models match that of the point dipole, as expected.

A still better insight in the behaviour of different models at small and intermediate distances can be achieved by visualising magnetic field lines. By definition, the elementary vector of the tangent to the field line,  $d\mathbf{L}$ , in each point of this line is parallel to the field vector. The vector product for parallel vectors vanishes, so, for the magnetic field lines we get  $d\mathbf{L} \wedge \mathbf{B} = \mathbf{0}$ . In cylindrical coordinates this reduces to  $dz/d\rho = B_z/B_\rho$ , and we get the following equation for the magnetic field lines:

$$z(\rho) = \int_{y=\rho_{\text{inf}}}^{\rho \leq \rho_{\text{sup}}} \frac{B_z(y, z)}{B_\rho(y, z)} dy, \quad (29)$$

where  $\rho_{\text{inf}}$  and  $\rho_{\text{sup}}$  are, respectively, the smallest and the largest value of  $\rho$  for a given field line, and  $z \in [\rho_{\text{inf}}, \rho_{\text{sup}}]$  is a dummy variable.

We have put forward a FORTRAN 77 computer code for calculating the magnetic field lines for different dipole models according to both the exact expressions and their Taylor expansions, see the appendix. Visualisation of the field lines calculated using the Taylor expansions allows to estimate contributions of various expansion terms and the general convergence of the Taylor series for different models.

In the current loop model the exact expressions of the magnetic field components, equation (20), are very complicated, so, we have chosen to compute them by numerical integration over the angle  $\varphi'$  of the elementary field components expressed through the Biot Savart law, see equation (1) and figure 2:

$$\begin{aligned} B_\rho &= \frac{\mu_0 m}{4\pi \pi R} \int_0^{2\pi} \frac{z \sin \varphi'}{(R^2 + \rho^2 - 2R\rho \sin \varphi' + z^2)^{3/2}} d\varphi', \\ B_z &= \frac{\mu_0 m}{4\pi \pi R} \int_0^{2\pi} \frac{R - \rho \sin \varphi'}{(R^2 + \rho^2 - 2R\rho \sin \varphi' + z^2)^{3/2}} d\varphi'. \end{aligned} \quad (30)$$

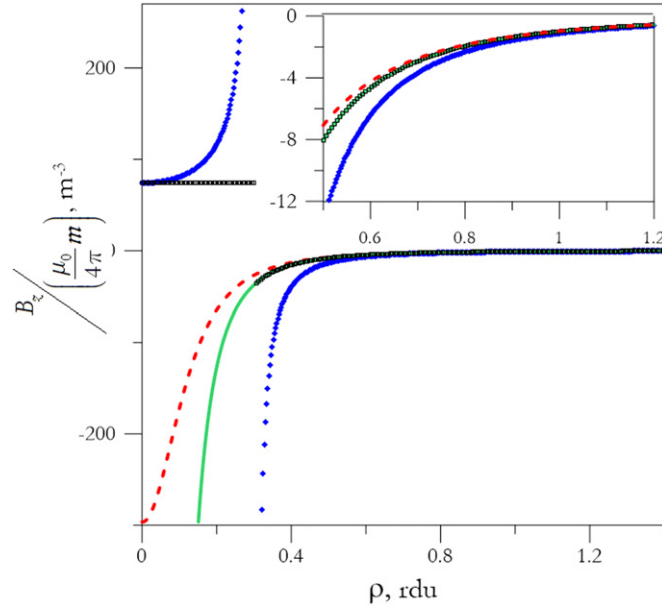


**Figure 4.**  $B_z(\rho, \vartheta = \pi/2)$  dependences for a uniformly magnetised sphere of radius  $R = 0.3$  rdu (circles, grey online), a circular current loop of radius  $R = 0.3$  rdu, (diamonds, blue online) and a pair of fictitious magnetic charges,  $d = 0.3$  rdu apart, (dashed, red online) compared do that of the point dipole (continuous, green online). The inset: shows a zoom in the behaviour of  $B_z$  at larger distances.

The corresponding exact expressions for the model of a pair of magnetic charges have been given in the previous section, see equation (26).

The Taylor expansions of the field line equation in the computer code have been obtained by expanding in the Taylor series the ratio  $B_z$  over  $B_\rho$ . For the model of a current loop this results in

$$\frac{B_z}{B_\rho} = \frac{2}{3} \frac{1}{\sin 2\vartheta} \left[ \begin{aligned} &3 \cos^2 \vartheta - 1 + \frac{1}{4}(5 \cos^2 \vartheta + 3)\varepsilon^2 - \frac{5}{32}(7 \cos^4 \vartheta - 6 \cos^2 \vartheta - 1)\varepsilon^4 \\ &+ \frac{5}{512}(203 \cos^6 \vartheta - 273 \cos^4 \vartheta + 65 \cos^2 \vartheta + 5)\varepsilon^6 \end{aligned} \right], \quad (31)$$

and for that of a pair of magnetic charges we get:

$$\frac{B_z}{B_\rho} = \frac{2}{3} \frac{1}{\sin 2\vartheta} \left[ \begin{aligned} &3 \cos^2 \vartheta - 1 - \frac{1}{12}(5 \cos^2 \vartheta + 3)\varepsilon^2 - \frac{1}{144}(7 \cos^4 \vartheta - 15 \cos^2 \vartheta)\varepsilon^4 \\ &- \frac{1}{1728}(26 \cos^6 \vartheta - 63 \cos^4 \vartheta + 45 \cos^2 \vartheta)\varepsilon^6 \end{aligned} \right]. \quad (32)$$

We remind the reader that in equations (31) and (32)  $\varepsilon$  has different meaning. In all cases, the numerical integration over  $\rho$  in equation (29) has been performed using the Runge Kutta method [8].

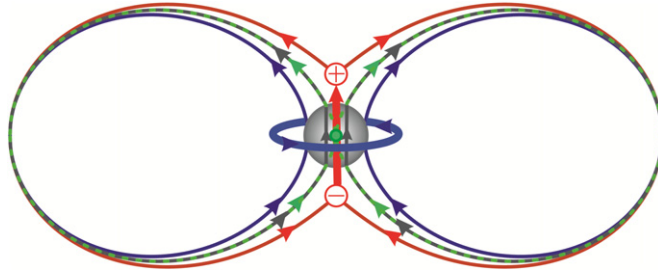


**Figure 5.** Magnetic field lines for different dipole models scaled in rdu. The external line (red online) corresponds to a pair of magnetic charges  $d = 0.75$  apart. The intermediate dashed (green online) and continuous (grey online) lines refer to a point dipole and uniformly magnetised sphere of radius  $R = 0.20$ , respectively. The internal line (blue online) is due to a current loop of radius  $R = 0.40$ . All the lines merge at the maximal distance  $r_{\max} = 2.0$ .

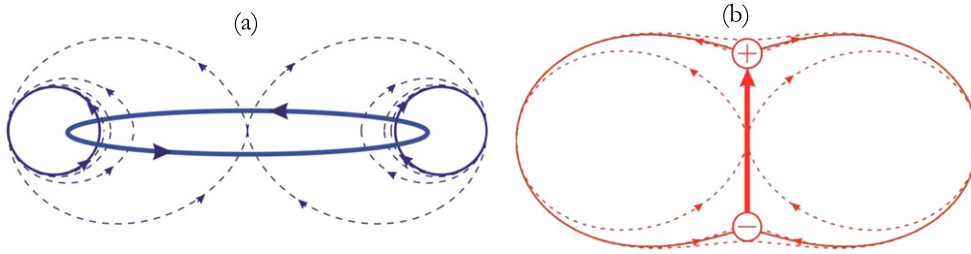


**Figure 6.** Magnetic field lines in the models of a current loop (a) and of a pair of magnetic charges (b) calculated using the exact expressions of the magnetic fields (continuous lines) and the Taylor expansions to the 0th, 2nd, 4th and 6th order in the corresponding small parameters. All the lines merge at the maximal distance  $r_{\max} = 2.0$  rdu. With increasing the expansion order, in (a) each subsequent field line remains confined inside the previous one, while in (b) it passes alternately from inside to outside of the exact field line profile.

With the aid of this programme we have visualised the field lines for all models, see figure 5. The calculations have been made using the exact expressions, *vide supra*, and the modelling parameters have been chosen in such a way that all the field lines ostensibly merge at the maximal distance  $r_{\max}$  from the source. As one can see, at distances comparable with the model size, the appearance of the field lines predicted by each model is totally different. The lines produced by a uniformly magnetised sphere are parallel to the dipole axis inside the sphere and coincide with those of the point dipole outside the sphere. The lines due to a current loop close on themselves inside the loop while those of a pair of magnetic charges diverge from the positive charge and converge towards the negative one. In all cases, at small distances the behaviour of the field lines has nothing in common with that expected for the point dipole, in which case the field lines close on themselves in the space origin.

In certain applications, e.g. in calculating the interaction energy between magnetic moments embedded in a condensed matrix, one needs a good approximation for the magnetic field produced at intermediate distances from the magnetic source. Obviously, in such cases in the multipole expansion, see equation (3), higher-order terms (quadrupole etc) should be maintained. Figure 6 compares the magnetic field lines calculated using the exact expressions

and Taylor expansions to different orders in the corresponding small parameter for the models of a circular current loop and a pair of fictitious magnetic charges. One can see that in the model of a current loop the expansion up to the 6th order in  $\varepsilon = R/r$  provides a good approximation for  $R/r_{\max} \leq 3/4$ , and in the model of a pair of magnetic charges the same expansion in  $\varepsilon = d/r$  already for  $d/r_{\max} = 3/4$  yields a result practically indistinguishable from that of the exact calculation.

## 7. Conclusions

In this work we have presented a consistent approach, based on the vector potential formalism, to the calculation of the magnetic field produced by different models of the magnetic dipole. Of course, exactly the same results could be obtained with the *scalar* magnetic potential. However, using the vector potential for calculating the magnetic field is more acceptable from the methodological and educational points of view. Indeed, in teaching electrostatics and magnetostatics, it is preferable to respect a certain ‘symmetry’, viz., to preserve ‘parenting relationships’ from the scalar potential to the electric field and from the vector potential to the magnetic field.

We have seen that all three models of the magnetic dipole considered in this study yield identical results at large distances. Indeed, the *first* terms of Taylor expansions of the magnetic field for both the models of a current loop and of a pair of magnetic charges coincide with the *exact* expression of the magnetic field outside the uniformly magnetised sphere. Therefore, such a sphere represents not only a perfect but also a quite physically realistic model of the point dipole.

However, starting from the second term in the Taylor series, the magnetic field in the models of a current loop and of a pair of magnetic charges totally diverge. Interestingly, for these models this divergence goes in opposite directions, so that the characteristics of the magnetic dipole models at small and intermediate distances become quite sensible to the choice of the dipole model. Our computer code allows visualising these discrepancies; besides, it gives the possibility of comparing the aspect of the magnetic field lines calculated using the exact expressions of the magnetic field and the corresponding approximate expressions obtained by expanding in Taylor series of different order.

## Appendix. Computer code for visualising field lines produced by different magnetic dipole models

---

```

C          Calculates magnetic field lines for the current loop and pair of charges models
C          with both exact expressions and Taylor expansions up to 6th order
C*****
          IMPLICIT DOUBLE PRECISION (a,h,p,z)
          DIMENSION zp( 10001: 10001), zn( 10001: 10001)
          COMMON/Parametres/me, N, y ( 10001: 10001), Pi, d,nea, nT
          COMMON /Angulaire/Sphi(1000), pas ang, Na
          Pi = dacos( 1d0)
C*****
C          me = 1: Current loop; me = 2: Pair of charges
C          nea = 1: Exact calculation;nea = 2: Taylor expansion
C          nT = 0, 2, 4, 6: order of Taylor expansion
C*****

```

(Continued.)

```
me = 1
nea = 1
nT = 2
C      d = loop radius for me = 1 and d = charge separation for me= 2.
      d = 1.5d0
C      y sup: maximal distance between the dipole and the observation point.
      y inf = 0.d0
      y sup = 2.0d0
C      Na: number of angles used in integrating the magnetic field over the loop
      Na = 90
      pas ang = 0.5d0*Pi/dble(Na)
C*****
C      Preparing the integration
      DO i = 1, Na
      phi = 36d1/dble(Na)*dble(i)
      Sphi(i) = dsind(phi)
      ENDDO
C*****
C      Discretising y
      N = 1000
      dN = dble(N)
      pas y = (y sup y inf)/dN
      DO j = 1, N
      y (j) = dble(j)*pas y
      ENDDO
C*****
C      Calculating the field line with Runge Kutta method
      j = N
C      Choosing an initial value of z (z > 0d0) to get a smooth aspect of the field line
      z = 0.01d0
      1      zp(j) = z
            zn(j) = z
            zp(j) = z
            zn(j) = z
            y1 = y (j)
            z1 = z
            CALL Ratio(y1, z1, a)
            z2 = z1 0.5d0*pas y*a
            y2 = y1 0.5d0*pas y
            CALL Ratio(y2, z2, b)
            z3 = z1 0.5d0*pas y*b
            CALL Ratio(y2, z3, c)
            z4 = z1 pas y*c
            y3 = y1 pas y
            CALL Ratio(y3, z4, dd)
            z = z pas y*(a + 2d0*b + 2d0*c + dd)/6d0
C      Continue calculating
      2      IF (j. gt. 0. and. z. gt. 0d0) THEN
            j = j - 1
            GOTO 1
            ENDIF
```

(Continued.)

```
C*****
C          Creating output file. zp and zn are the upper and lower parts of the field line.
C          Give an appropriate file name!
C          OPEN(2,file = 'Cur loop d = 1.5 exact.txt')
C          DO j = N, N
C          WRITE (2, 3) y (j), zp(j), zn(j)
C          ENDDO
C          3      FORMAT (3E24.6)
C          CLOSE(2)
C          99     END
C*****
C          SUBROUTINE Ratio (y, z, rat)
C          Implements the Runge Kutta procedure
C*****
C          IMPLICIT DOUBLE PRECISION (a h, p z)
C          DIMENSION rT(0: 6)
C          COMMON/Parametres/me, N, y ( 10001: 10001), Pi, d, nea, nT
C          COMMON/Angulaire/Sphi(1000), pas ang, Na
C*****
C          IF (nea. eq. (1)) THEN
C          Exact calculation
C          IF (me. eq. (1)) THEN
C          Current loop: integrating the magnetic field over the loop
C          By = 0d0
C          Bz = 0d0
C          DO i = 1, Na
C          rpm = (y**2 + z**2 2d0*d*y*Sphi(i) + d**2)**1.5
C          dBy = 1d0/Pi/d*z*Sphi(i)/rpm
C          dBz = 1d0/Pi/d*(d y*Sphi(i))/rpm
C          By = (By + dBy*pas ang)
C          Bz = (Bz + dBz*pas ang)
C          ENDDO
C*****
C          ELSEIF (me. eq. (2)) THEN
C          Pair of charges
C          rm = ((z 0.5d0*d)**2 + y**2)**1.5
C          rp = ((z + 0.5d0*d)**2 + y**2)**1.5
C          Bz = (z 0.5d0*d)/rm (z + 0.5d0*d)/rp
C          By = y*(1d0/rm 1d0/rp)
C*****
C          ENDIF
C          rat = Bz/By
C*****
C          ELSEIF (nea. eq. (2)) THEN
C          Taylor expansion
C          z2 = z*z
C          z4 = z2*z2
C          y2 = y*y
C          y4 = y2*y2
C          r2 = y2 + z2
```

(Continued.)

---

```
P0 = (2d0*z2 y2)/(y*z)
P2 = (3d0*y2 + 8d0*z2)/(r2*y*z)
C*****
IF (me. eq. (1)) THEN
C
  Current loop
  z00 = 1d0/3d0*P0
  z02 = 1d0/12d0*P2*d**2
  z04 = 5d0/96d0*(y2 + 8d0*z2)*y/(r2**3*z)*d**4
  z06 = 5d0/1536d0*(5*y4 + 80d0*y2*z2 128d0*z4)*y/(r2**5*z)*d**6
C*****
ELSEIF (me. eq. (2)) THEN
C
  Pair of charges
  z00 = 1d0/3d0*P0
  z02 = 1d0/36d0*P2*d**2
  z04 = 1d0/432d0*z*(15d0*y2 + 8d0*z2)/(r2**3*y)*d**4
  z06 = 1d0/5184d0*z*(45d0*y4 + 27d0*z2*y2 + 8d0*z4)/(r2**5*y)*d**6
C*****
ENDIF
C
nT = 0, 2, 4, 6: order of Taylor expansion
rT(6) = z00 + z02 + z04 + z06
rT(4) = z00 + z02 + z04
rT(2) = z00 + z02
rT(0) = z00
rat = rT(nT)
ENDIF
RETURN
END
```

---

## References

- [1] Jackson J D 1998 *Classical Electrodynamics* 3rd edn (Hoboken, NJ: Wiley)
- [2] Griffiths D J 1999 *Introduction to Electrodynamics* 3rd edn (Upper Saddle River, NJ: Prentice Hall)
- [3] Bezerra M, Kort Kamp W J M, Cougo Pinto M V and Farina C 2012 How to introduce the magnetic dipole moment *Eur. J. Phys.* **33** 1313
- [4] Landau L D and Lifshitz E M 1971 *The Classical Theory of Fields* 3rd edn (Oxford: Pergamon)
- [5] Curie P 1894 Sur la symétrie dans les phénomènes physiques, symétrie d'un champ électrique et d'un champ magnétique *J. Phys.* **3** 393
- [6] Arfken G B, Weber H J and Harris F E 2012 *Mathematical Methods for Physicists* 7th edn (Waltham, MA: Academic)
- [7] Dirac P A M 1931 Quantised singularities in the electromagnetic field *Proc. R. Soc. A* **133** 60
- [8] Atkinson K E 1989 *An Introduction to Numerical Analysis* 2nd edn (New York: Wiley) p 420 ff